Computational optimization of the dual-mode dual-fuel concept through genetic algorithm at different engine loads

Energy Conversion and Management
Volume 208, 15 March 2020, 112577
https://doi.org/10.1016/j.enconman.2020.112577

Guangfu Xu [a], Javier Monsalve-Serrano [b], Ming Jia [a, *], and Antonio García [b]

[a] Key Laboratory of Ocean Energy Utilization and Energy Conservation of Ministry of Education, Dalian University of Technology, Dalian, 116024, P.R. China

[b] CMT - Motores Térmicos, Universitat Politècnica de València, Camino de Vera s/n, 46022 Valencia, Spain

Abstract

The diesel/gasoline dual-mode dual-fuel (DMDF) combustion concept was optimized in a compression-ignition engine by combining the computational fluid dynamics (CFD) simulations with the genetic algorithm. Seven operating parameters with remarkable influences on the engine performance were chosen as the variables to be optimized for simultaneously minimizing the fuel efficiency, nitrogen oxides (NO_x), and soot emissions. Moreover, the potential of the further improvement of the DMDF combustion concept was discussed, and the rationality of this strategy was demonstrated. The results indicate that, at low load, simultaneous improvement of the fuel economy and emissions can be realized by strengthening the homogeneous combustion. At mid load, the fuel economy can be improved by reducing the heat transfer losses, while the NO_x emissions are sacrificed to some extent. At high load, improved fuel economy can be realized by transferring a part of diffusion combustion to premixed reactivity-controlled compression ignition (RCCI) combustion. Concerning the operating parameters, lower intake temperature is beneficial to decrease the transfer losses, and the control of intake temperature is crucial for the stable operation of DMDF combustion under wide load conditions. Overall, gross

indicated thermal efficiency above 45% is achieved, and the NO_x and soot emission can be maintained under the Euro 6 standard for the test load range.

Keywords: Dual-mode dual-fuel (DMDF); Numerical simulation; Genetic algorithm; EURO VI emission standards; Fuel efficiency

1 Introduction

With the gradually stringent emission and fuel consumption regulations, further eliminating the engine-out emissions and improving fuel efficiency are necessary for present diesel engines. Up to now, the after-treatment devices have demonstrated their capabilities of decreasing the engine-out emissions. However, these devices may arise the challenges of increased cost and fuel consumption [1, 2]. In order to solve the emission problems fundamentally and effectively, the low-temperature combustion (LTC) strategy is being investigated recently. These concepts all feature low-temperature and homogeneous-mixing, which are beneficial for reducing the nitrogen oxides (NO_x) and particular matter (PM). Among different LTC strategies, reactivity controlled compression ignition (RCCI) mode exhibits more flexible control of the combustion behavior by utilizing the dual-fuel system. For this reason, the investigation of the RCCI mode attracts increasing attention recently [3-6].

The dual-fuel RCCI combustion mode is accomplished by premixing a low-reactivity fuel in the intake port and directly injecting a high-reactivity fuel into the cylinder. Thus, the in-cylinder fuel/air mixture reactivity can be tuned, which provides a greater control degree of the heat release rate (HRR) than the other LTC modes [2, 7]. Furthermore, the separate fuel supply strategy can lead to the reactivity stratification of the in-cylinder charge. As a result, the HRR can be effectively controlled. This enables to extend the operation towards the high load. Even so, the application of the RCCI combustion in full-load operation is still difficult. At low load, the lean combustion can increase the unburned products and deteriorates fuel efficiency [8]. At high load, the engine noise turns into the

65 main restriction for the RCCI operation [2, 9]. Furthermore, in spite of the reactivity stratification, the RCCI mode
66 is still kinetically controlled and very sensitive to the intake conditions [10, 11].

67 Up to now, some efforts have been made to extend the RCCI operation range. By optimizing the fuel injection
68 parameters of a gasoline/diesel RCCI engine focusing on high load, Lim et al. [3] found that a gross indicated mean
69 effective pressure (IMEP) of 21 bar was reached by employing the double-direct injection of diesel. At the same
70 time, extremely low NO_x and soot emissions were achieved while the indicated thermal efficiency of 48.7% can be
71 attained. In the study of Dempsey and Reitz [12], by employing the optimized piston with a reduced compression
72 ratio, the high peak pressure rise rate (PPRR) limit can be met at high load. Moreover, stable and satisfied RCCI
73 combustion can be accomplished from 4 to 23 bar IMEP. Furthermore, the optimized piston was also utilized for
74 the RCCI operation at high load [13, 14].

75 Molina et al. [15] extended the operating range of RCCI combustion by applying the Miller cycle with
76 multiple injections. At low load, the dual injection strategy was coupled with a high premix ratio (PR) for
77 controlling the combustion phasing and emissions. At mid load, a lower effective compression ratio was needed for
78 managing the in-cylinder thermodynamic conditions and auto-ignition. At high load, a single injection of diesel was
79 utilized to trigger the ignition and reduce the pressure rise rate. Furthermore, Benajes et al. [16] introduced a
80 dual-mode dual-fuel (DMDF) strategy, in which a switch from RCCI combustion to diffusive combustion was
81 employed for full-load operation. At lower loads, the fully-premixed homogeneous charge compression ignition
82 (HCCI) or highly-premixed RCCI combustion was introduced for decreasing the emissions and improving fuel
83 efficiency. At higher loads, the in-cylinder charge combustion shifts to the diffusive dual-fuel combustion for
84 satisfying the engine mechanical requirements, which sacrifices the NO_x and soot emissions to some extent
85 compared to the lower part of the engine map.

From Ref. [16], it can be summarized that the DMDF combustion strategy has exhibited the pleasant performance, especially for extending the operating condition of the dual-fuel combustion. However, because the present operating parameters were empirically obtained from the experiment, the DMDF strategy was not operated in the optimum region under the various conditions. Thus, there still exists improvement space to be excavated for the DMDF strategy, especially for the combustion and emission performance at high load. For further strengthening the performance of DMDF strategy aiming at meeting the current emission and fuel consumption standards, systematic optimization of the key operating parameters deserves to be performed.

In this study, based on the experiments conducted by Benajes et al. [16], further optimization of the DMDF combustion was conducted by employing the numerical simulations based on computational fluid dynamics (CFD) simulation and genetic algorithm. The objective of this work is to meet the Euro 6 emission limits and achieve high fuel efficiency by optimizing the DMDF combustion process. First, the operating parameters with significant impact on the DMDF combustion were optimized. Then, the potential of the improvement of the DMDF combustion was discussed. Finally, the fuel energy path of the strategies obtained from the optimization process were analyzed to understand the reasons of the gains observed.

2 Computational methods

2.1 Computational model

The CFD code, an enhanced KIVA-3V [17], was employed for predicting the engine in-cylinder working process. The improved turbulence model, i.e., the generalized re-normalized group (GRNG) k-ε model [18], was used for modeling the flow in the cylinder. The spray impingement model was updated by Zhang et al. [19] for modeling the early in-cylinder fuel injection conditions. The liquid film model [20] was improved for better modeling the film evolution and vaporization. The quasi-dimensional vaporization model was used to model the

vaporization processes of fuel droplets [21] and liquid films [22]. In addition, the models of simulating the wall heat transfer [23], droplet collision [24], and droplet breakup [25] were also utilized in this study. The fuel chemistry was calculated by integrating the CHEMKIN solver [26] with the KIVA-3V code. The skeletal chemical mechanism of *n*-heptane and *iso*-octane proposed by Chang et al. [27] was applied to predict the ignition and combustion of the diesel fuel and gasoline fuel, respectively. These models have been extensively validated focusing on RCCI combustion in previous works from the Refs. [28, 29].

Table. 1 Engine specifications

Bore (mm)	110.0
Stroke (mm)	135.0
Connecting rod length (mm)	212.5
Geometric compression ratio	14.4:1
Swirl Ratio at IVC	2.3
Direct injection system	Common rail
Nozzle hole number	7
Included spray angle (°)	150
Nozzle hole diameter (mm)	0.177

The investigated engine is a medium-duty single-cylinder diesel engine [16]. The specifications of the test engine can be found in Table 1. For extending the RCCI operation region, the geometric compression ratio was decreased from 17.5:1 to 14.4:1 [16]. To save the computational time, a $1/7^{th}$ sector mesh was used, which corresponds to the domain with one nozzle hole. The process from the intake valve closing (IVC) to the exhaust valve opening (EVO) was taken into account in this study. The computational mesh is shown in Fig. 1. For the test engine, the bowl geometry was specially optimized for RCCI combustion in order to decrease the heat transfer losses and enhance the burning of the premixed fuel in the crevice region [16, 30]. Moreover, to accomplish the DMDF combustion in this work, the diesel fuel is provided by double direct injection, while the gasoline is premixed with the intake air in the intake port.

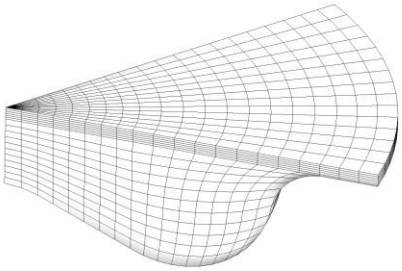

Fig. 1. Computational mesh.

Table 2. Specifications of the baseline cases

	Low-Base	Mid-Base	High-Base
IMEP (bar)	5.9	12.0	20.0
Engine speed (rev/min)	1200	1200	1200
p_{ivc} (bar)	1.60	2.32	3.09
T_{ivc} (K)	332.63	347.88	356.10
EGR rate (%)	19.71	50.17	31.01
SOI1 (°CAATDC)	-48.00	-45.00	-
SOI2 (°CAATDC)	-41.86	-5.00	6.00
MF1 (%)	51.91	36.84	-
PR (%)	89.51	62.10	33.95

Based on the experiments conducted by Benajes et al. [16], the validation of the computational model is first conducted. Three typical baseline cases are chosen for the validation with an IMEP of 5.9, 12.0, and 20.0 bar, which represents the low, mid, and high loads of the DMDF combustion, respectively. Consistently with the experiment, the engine speed is kept at 1200 rev/min. Table 2 lists the detailed specifications of the three baseline cases. At low load, the fully premixed RCCI combustion mode was applied, which was realized by premixing a large fraction of the gasoline combined with advanced double direct injections of the diesel fuel. At mid load, the highly premixed RCCI combustion mode was employed. In this case, a relatively lower premix ratio of gasoline was used. Meanwhile, the double diesel injections were also utilized, in which the second diesel injection was retarded near top dead center (TDC). At high load, a switch to the dual-fuel diffusion combustion is accomplished

by a further lower premix ratio combined with a retarded single diesel injection.

Fig. 2 compares the predicted and measured in-cylinder pressure and heat release rate (HRR) traces for the three baseline cases. As can be found, the simulated results have a good agreement with the measurements. This indicates that the present model can accurately predict the combustion process and capture the combustion characteristics of the DMDF concept at different loads. Fig. 3 demonstrates the comparisons of the emissions between prediction and measurement. It is seen that the quantitative predictions of the CO and soot emissions are still challenging. This is primarily owing to the complicated fuel/air mixing process, the deficiencies in the chemical mechanism [31], and the uncertainties in the measurements [2]. Since the overall trends of emissions can be well estimated, the current model is further utilized in the following study for engine optimization.

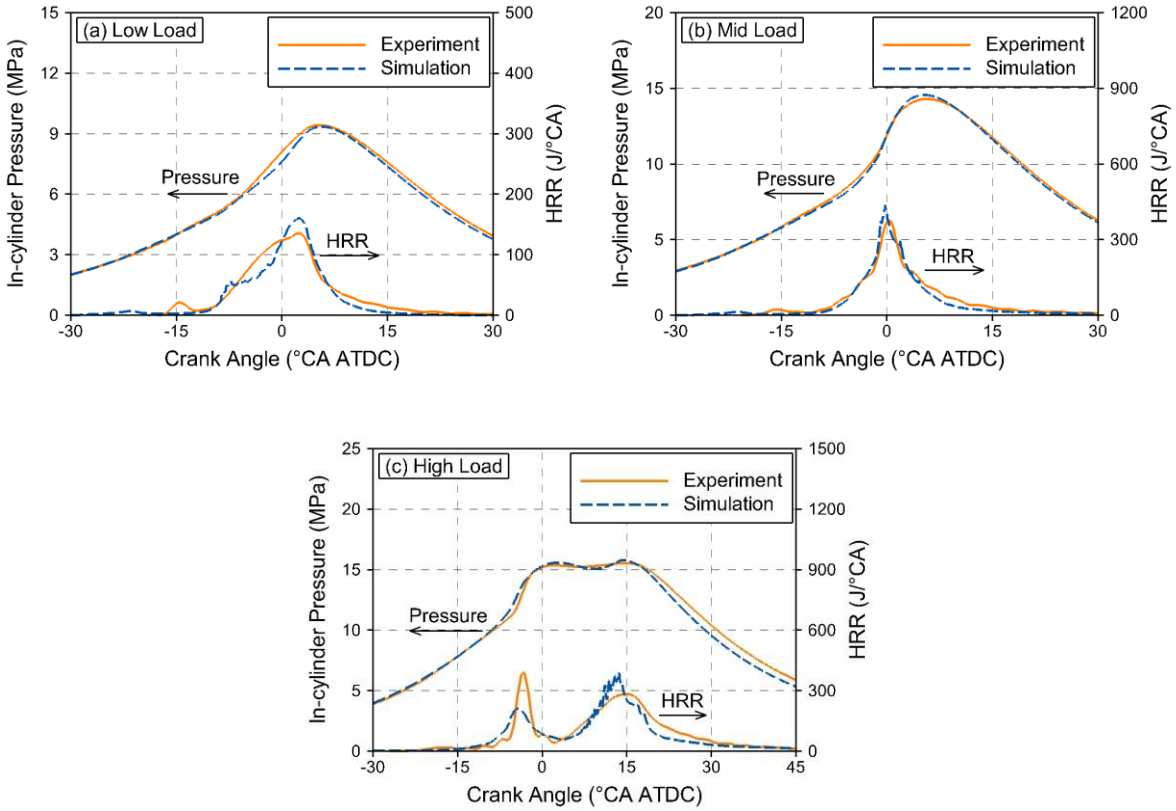

Fig. 2. Validation of the pressure and HRR for the baseline cases.

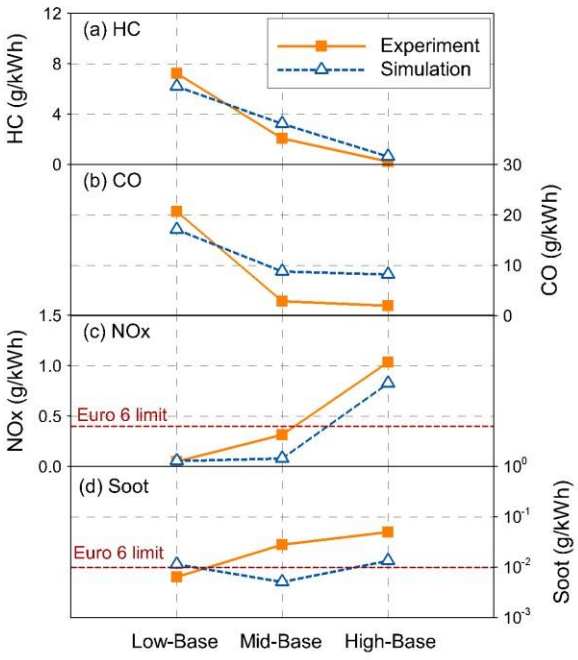

Fig. 3. Validation of the emissions for the baseline cases.

2.2 Optimization method

The DMDF combustion performance is considerably influenced by the relevant operating parameters. Manual optimization by modifying the parameters experimentally in the test engine is very time-consuming. Meanwhile, there exist trade-off relationships among the engine performance and emission parameters. Thus, in order to simultaneously minimizing the emissions and fuel consumption from DMDF combustion, the non-dominated sorting genetic algorithm II (NSGA-II) [32] was employed combined with the updated KIVA-3V. In the previous studies [13, 28, 33], the computational framework has been applied for the optimization of different combustion concepts, and its capability of searching for optimal cases was well demonstrated.

Table 3. Optimization specifications

Variables	Range
Premix Ratio	(0.0, 1.0)
SOI1 (°CA ATDC)	(-80.0, 10.0)
SOI2 (°CA ATDC)	(SOI1, 10.0)
Fraction of SOI1	(0.0, 1.0)
EGR	(0.0, 1.0)
T_{ivc} (K)	(300.0, 450.0)
p_{ivc} (bar)	(1.0, 4.0)

Consistently with the validation cases mentioned above, the optimization was performed at low, mid, and high loads with an IMEP of 5.9, 12.0, and 20.0 bar, respectively. The specifications of the optimization can be found in Table 3. Seven operating parameters with critical influences on the DMDF combustion are selected as variables to be optimized, including the premixed gasoline fraction (*i.e.*, premix ratio, PR), the injection timings of the diesel fuel (*i.e.*, SOI1 and SOI2), the mass fraction of the first diesel injection (*i.e.*, MF1), the EGR rate, and the in-cylinder temperature and pressure at IVC timing (*i.e.*, T_{ivc} and p_{ivc}). It should be noted that, in order to include all the rational cases in the final optimization solutions, the variation ranges of the operating parameters are relatively large, as shown in Table 3.

To evolve the population into low-emission and high-efficiency orientation, the gross EISFC, NO_x and soot emissions were selected as the optimization targets. Since two kinds of fuels with different lower heating values (LHV) were utilized, the equivalent indicated specific fuel consumption (EISFC) is introduced to evaluate the fuel efficiency [33], which is calculated as:

(1)

(2)

where m_{diesel} and $m_{gasoline}$ are respectively the mass of diesel and gasoline fuel; LHV_{diesel} and $LHV_{gasoline}$ are respectively the LHV of diesel and gasoline; W_i is the indicated work; p and V are respectively the pressure and volume in the cylinder; and E_{fuel} is the total energy of the fuel mixture supplied per cycle, which is fixed at each load in the optimization in this study.

Furthermore, several indicators were restricted to exclude irrational cases during the optimization calculation. To prevent the engine knock, the maximum pressure (p_{max}) and PPRR were restricted under 19.0 MPa and 15.0 bar/°CA, respectively [16]. Meanwhile, the ringing intensity (RI) was limited under 10 MW/m^2. The maximum temperature was kept above 1100 K to avoid misfire. The EISFC was restricted below 250 g/kWh to avoid fuel efficiency deterioration. The NO_x and soot emissions are limited under the Euro 6 emission standards, *i.e.*, 0.4 and 0.01 g/kWh, respectively.

3 Results and discussion

3.1 Global optimization results

To investigate the global optimization process, the evolution of the objectives and the variables at each load are first illustrated. Fig. 4 demonstrates the distributions of soot, NO_x, and EISFC of all the cases during the

optimization process at the three loads. From Fig.4, it can be found that a significant trade-off relationship can be observed between soot and NO_x, as well as between EISFC and NO_x emissions. Moreover, the color represents the generation number for each case, and the optimization degree increases with a deeper color. It can be found that the cases gradually move to the origin point with the optimization processing. This indicates that the soot and NO_x emissions, as well as the EISFC, are simultaneously reduced after the optimization.

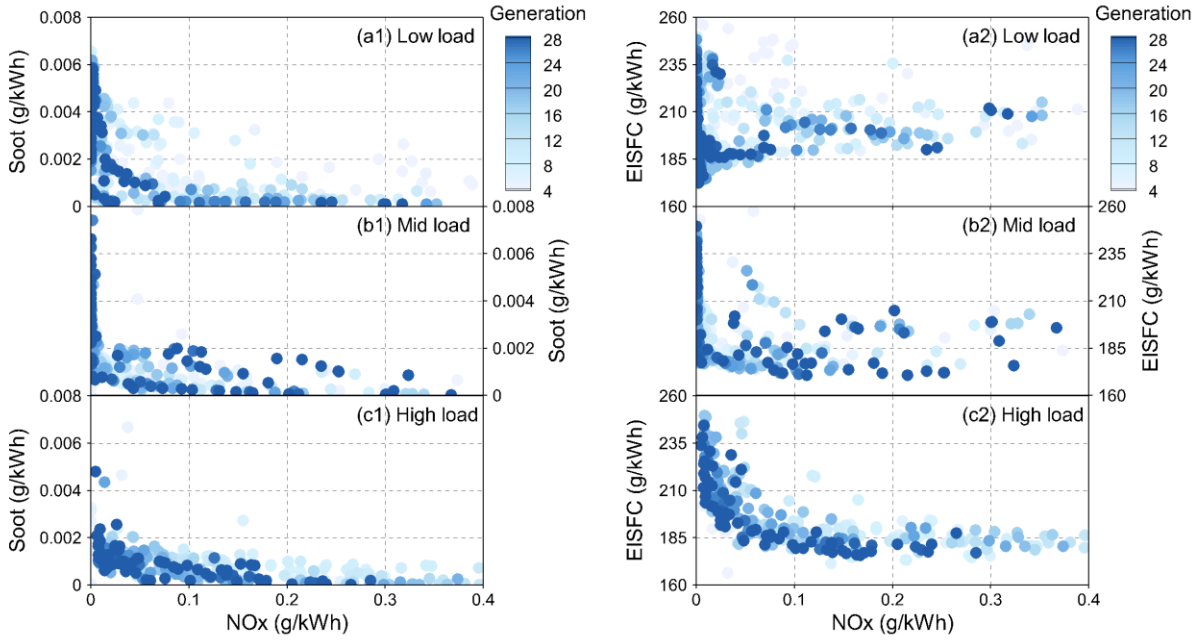

Fig. 4. Distributions of objectives of all the citizens at each load.

Among the cases generated during the optimization calculation, the final optimal cases with superior performance are selected and summarized. As depicted in Fig. 5, the blue, red, and green symbols denote the optimal cases obtained from the optimization calculation at low, mid, and high load, respectively. As can be observed, the soot and NO_x emissions of the optimal cases are capable of meeting the Euro 6 limits, *i.e.*, 0.01 g/kWh and 0.4 g/kWh, respectively. At the same time, the EISFC and PPRR are lower than 180 g/kWh and 15 bar/°CA, respectively. This indicates that pleasant performance is achieved while the stable operation is realized for the DMDF combustion strategy from the optimization process.

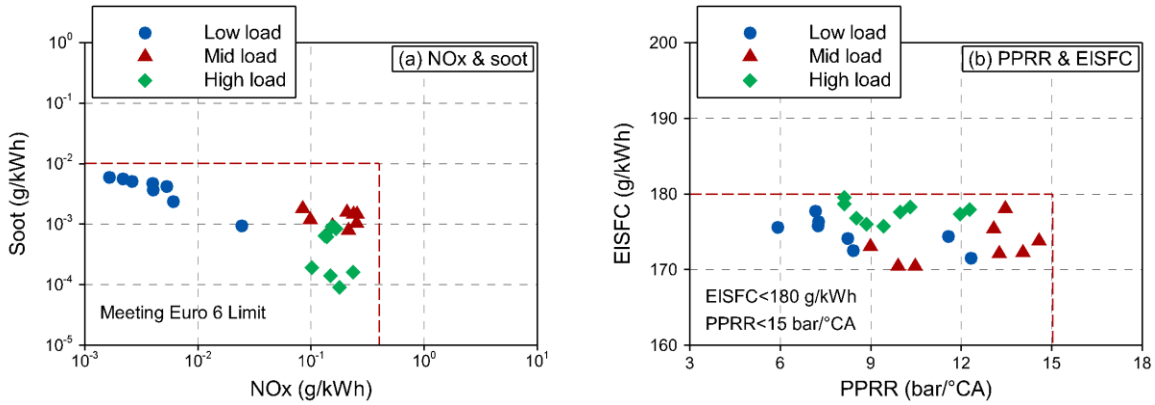

Fig. 5. Soot, NO_x, EISFC, and PPRR of the optimal cases.

Figs. 6 and 7 illustrate the fuel supply parameters of the optimal cases at each load. Fig. 6 shows the distribution of the direct diesel injection timings. The optimal cases are represented by solid symbols with different colors. As comparison, the baseline cases are also illustrated as represented by the hollow symbols. As mentioned above, the double injection strategy was utilized in the DMDF combustion. Thus, the second start of injection (SOI2) timing of diesel is kept after the first start of injection (SOI1) in the optimization calculations, as defined in Table 3. At low load, the SOI1 timing locates within -70~-45 °CA ATDC, and the SOI2 timing is around -45~-20 °CA ATDC. Compared to the Low-Base case, the optimal cases at low load utilize a relatively earlier SOI1 timing. This can promote the formation of homogeneous in-cylinder charge. At mid load, although both injection timings are retarded, the SOI2 timings of the optimal cases are relatively earlier than that the Mid-Base case. Thus, the injection and combustion events are decoupled to provide enough timing for the fuel/air mixing.

At high load, since the High-Base case employs a single injection strategy, the case is not presented in Fig. 6. For the optimal cases, the SOI2 timing is further retarded to prohibit an excessively advanced combustion phasing, as demonstrated in Fig. 6. According to the distributions of the diesel injection timings, the optimal cases can be categorized into two groups at high load, *i.e.*, Group 1 and Group 2, as shown in Fig. 6. In the cases of Group 1, the isolated fuel injections, *i.e.*, an earlier SOI1 and a later SOI2, are utilized. On the contrary, the closer two fuel

injection timings, *i.e.*, a later SOI1 and a relatively earlier SOI2 are introduced in the cases in Group 2. By analyzing the cases at high load, it is observed that the cases of both the two groups exhibit very similar performance. For simplicity, only the cases in Group 1 are selected to represent the optimal cases at high load in the following parts. It should be noted that the SOI2 timings of the optimal cases in Group 1 are similar to the SOI timing of the High-Base case.

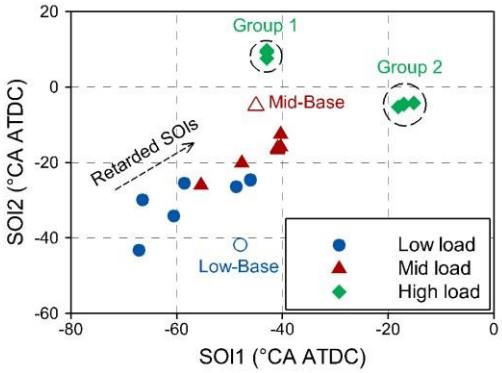

Fig. 6. Diesel fuel injection timings of the optimal cases at the three loads.

Fig. 7 illustrates the fuel supply fractions of the premixed gasoline and the directly injected diesel for the optimal cases, including the premix ratio (PR) and the mass fraction of the first diesel injection (MF1). As seen, the PRs of the optimal cases are all above 0.9 at low load, which is identical with the Low-Base case. This indicates that a large fraction of fuel supplied by premixing gasoline in the intake port. Meanwhile, compared to the Low-Base case, the MF1s of the optimal cases are close to 1.0 at low load. This means that nearly all the diesel fuel is provided in the first injection well before TDC (see Fig. 6). Thus, the fully premixed RCCI combustion is accomplished at low load. When load elevates to mid load, both the PR and MF1 are decreased under 0.6, which is used to prohibit advanced combustion phasing and high PPRR. At high load, the MF1 is further decreased. Meanwhile, since the SOI2 timing of diesel is also retarded (see Fig. 6), the combustion phasing can be well controlled. Thus, a relatively larger amount of gasoline fuel can be premixed at high load compared to the

High-Base case, as illustrated in Fig. 7. Overall, the optimal cases at each load indicate that, for the optimized DMDF strategy, the combustion process mainly features the RCCI combustion characteristics at low and mid loads, while the diffusion combustion becomes important at high load.

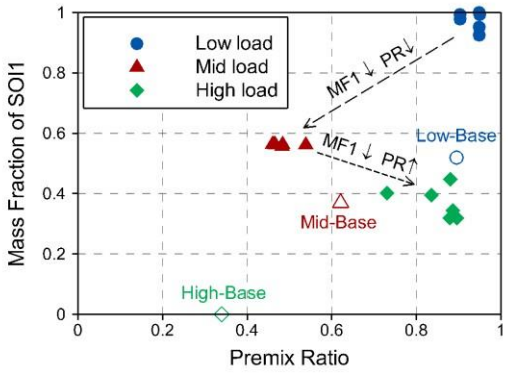

Fig. 7. Mass fraction of the first diesel injection and premixed ratio of the optimal cases at the three loads.

The parameters describing the intake conditions for the optimal cases are demonstrated in Fig. 8. The intake conditions include the initial in-cylinder temperature (T_{ivc}) and pressure (p_{ivc}) at IVC timing, as well as the EGR rate. Consistently, the optimal cases are respectively denoted by the blue, red, and green solid symbols, and the baseline cases are represented by the hollow symbols. It is observed that the initial pressure at IVC timing increases with increasing load. This indicates that the intake pressure must be increased at higher loads to provide adequate oxygen for the fuel combustion, as indicated in Refs. [34, 35]. As for the EGR rate, it can be found that a lower value is utilized at low load, as illustrated in Fig. 8(a). This is because that the combustion temperature is relatively low owing to the lean combustion at low load, which weakens the need of EGR for decreasing the NO_x emissions. However, at mid load, the total fuel energy and concentration increase with the increasing fuel amount, which enhances the potential of high combustion temperature. Therefore, the EGR rate should be elevated to control the ignition timing and the NO_x emissions. At high load, the fuel injections are retarded (see Fig. 6), especially for the SOI2 timing, which dominates the combustion phasing [36]. As a result, the combustion phasing and temperature

can be well managed, and a relatively lower EGR rate is needed. Moreover, it can be found that the EGR rate and the p_{ivc} of the optimal cases are consistent with those of the baseline cases.

Fig. 8(b) illustrates the in-cylinder initial temperature at IVC timing (T_{ivc}) of the optimal cases at each load. It is observed that, at low load, a higher T_{ivc} is required for promoting the combustion and increase the combustion efficiency. On the contrary, different with the baseline cases at mid and high loads, a relatively reduced T_{ivc} is utilized for the optimal cases, in order to avoid advanced ignition and overly high PPRR. Overall, the control of intake temperature is very crucial for the stable operation of the DMDF combustion at wide load ranges.

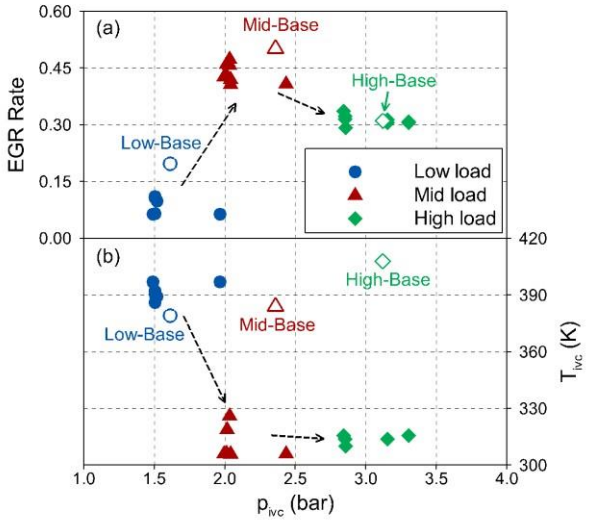

Fig. 8. T_{ivc} and EGR rate of the optimal cases at the three loads.

3.2 Discussion of the representative cases

3.2.1 Performance of the representative cases

To further investigate the performance of the final optimal results, several typical cases are selected and discussed at each load including the Low-Optimal, Mid-Optimal, High-Optimal1, and High-Optimal2 cases. In order to demonstrate the improvement achieved in the optimization calculation, the baseline cases (coming from the experiments) are also illustrated for comparison. The operating parameter specifications of the four representative optimal cases are shown in Table 4. Furthermore, Fig. 9 summarizes the fuel supply strategies of the

optimal cases compared to the baseline cases, including the diesel fuel injection timings and the fuel supply fractions. For every single bar, the axial location represents the injection timing, while the bar size denotes the ratio of the fuel energy in each injection event to the total input energy per cycle. The orange bars represent the fuel supply strategies of the baseline cases, and the blue and green bars represent those of the optimal cases.

Table 4. Operating parameters of the representative optimal cases

	Low-Optimal	Mid-Optimal	High-Optimal1	High-Optimal2
p_{ivc} (bar)	1.51	1.99	3.30	3.39
T_{ivc} (K)	392.16	306.12	315.52	304.35
EGR (%)	6.45	42.67	30.50	31.35
SOI1 (°CAATDC)	-60.56	-40.32	-42.89	-33.49
SOI2 (°CAATDC)	-34.18	-15.95	7.61	8.22
MF1 (%)	99.38	56.32	44.73	43.51
PR (%)	94.96	46.07	88.10	33.39

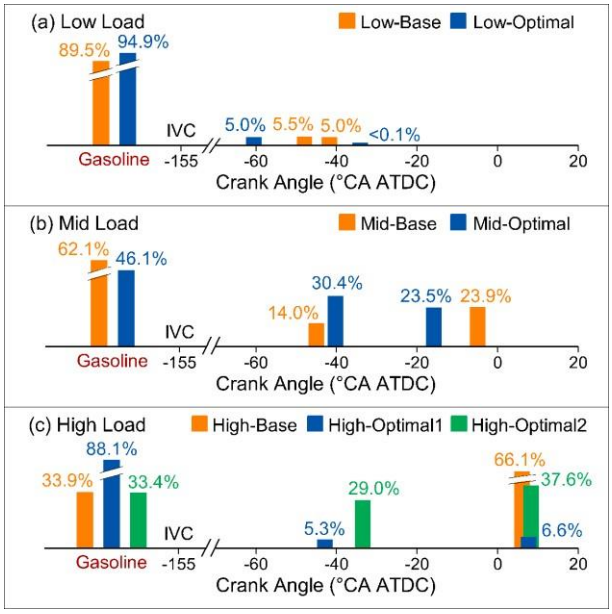

Fig. 9. Fuel supply strategies of the optimal cases and baseline cases.

As seen in Fig. 9(a), the PR is increased for the Low-Optimal case compared to the baseline case. Meanwhile, the injected diesel mass in the second injection is extremely lower in contrast to the first diesel injection. This indicates that the second injection of diesel can be omitted, and a single injection with relatively earlier injection timing is sufficient for realizing the fully premixed RCCI combustion mode at low load. At mid load, the premix

ratio is decreased to some extent compared to that of low load. Compared to the Mid-Base case, the MF1 is increased and the SOI2 timing is advanced to some extent for the Mid-optimal case, as illustrated in Fig. 9(b).

Fig. 9(c) demonstrates the fuel supply strategies of the optimal cases at high load, in which two optimal cases are chosen to be compared to the High-Base case. As shown in Fig. 9(c), for the High-Base case, a relatively lower PR is used, and a larger fraction of diesel fuel is injected after TDC with a single injection strategy. In the High-Optimal1 case, a higher PR is employed, and the mass of the direct-injected diesel is significantly decreased. Moreover, an advanced SOI1 timing is employed for the High-Optimal1 case, while the SOI2 timing is after TDC. For comparison, a compromised case with lower PR and double direct injection strategy was manually designed, which is named as High-Optimal2. This case was created based on a case in the previous generation during the optimization process to fulfill the PPRR limit. In the High-Optimal2 case, a similar PR is employed compared to the High-Base case. However, the large amount of injected diesel fuel is divided into two parts. A portion of the diesel fuel is injected before -30 °CA ATDC, while the second fuel injection is kept after TDC as well.

3.2.2 Combustion Behaviors of the Optimal cases

The combustion characteristics are further investigated in this section. Fig. 10 shows the in-cylinder pressure and HRR traces of the optimal and baseline cases. As demonstrated in Fig. 10(a), the HRR and pressure rise rate are significantly increased and the combustion duration is decreased after the optimization. This is owing to the fact that the Low-Optimal case uses higher PR and higher initial temperature compared to the Low-Base case. Thus, the heat release rate is accelerated, which is helpful for improving the low-load fuel economy (see Fig. 13(a)). As illustrated in Fig. 10(b), at mid load, although some discrepancies in the MF1 and SOI1 timing exist between the Mid-Optimal and Mid-Base cases, the combustion process of both cases is similar. Compared to the Mid-Base case, the maximum HRR and PPRR are decreased for the Mid-Optimal case, which is mainly due to the reduced premix

ratio.

Fig. 10(c) further compares the pressure and HRR traces of the optimal cases and baseline cases at high load. As can be observed, both the High-Base and High-Optimal2 cases exhibit the two-stage combustion characteristics. For the High-Base case, the first combustion stage starts with the reaction of the premixed gasoline fuel. Then, the second combustion stage starts with the diesel injection after TDC, promoting the diffusion combustion of the diesel fuel. For the High-Optimal2 case, as a large fraction of the diesel fuel is provided before -30 °CA ATDC (see Fig. 9(c)), the in-cylinder charge reactivity is high enough for auto-ignition before the second diesel injection, leading to diesel/gasoline RCCI combustion firstly. Then, the second fuel injection results in the diffusion combustion of the diesel fuel, resulting in the second combustion stage. Compared to the High-Base case, by transferring a portion of the diesel fuel from the diffusion combustion into the premixed RCCI combustion, the diffusion combustion fraction is reduced for the High-Optimal2 case. This is beneficial to improve the fuel economy and reduce NO_x and soot emissions. It is worth noting that, for the High-Optimal2 case, although a relatively lower T_{ivc} is used for avoiding an excessively advanced ignition, the PPRR is still relatively higher and close to the PPRR limit (*i.e.*, 15 bar/°CA), as denoted in Fig. 10(c).

In the High-Optimal1 case, the combustion phasing is well retarded after TDC due to utilizing a higher PR and a lower T_{ivc},. In this case, the large-fraction of premixed gasoline and the diesel fuel in the first injection event lead to the premixed RCCI combustion. Meanwhile, the lower T_{ivc} is employed for controlling the ignition timing of the premixed RCCI combustion after TDC. Moreover, the residual diesel is injected exactly during the RCCI combustion process. Thus, the diffusion combustion of the post-injected diesel and the RCCI combustion occur simultaneously. Therefore, the High-Optimal1 case exhibits a nearly one-stage combustion process, as shown in Fig. 10(c). In summary, compared to the High-Base and High-Optimal2 cases, the diffusion combustion fraction is

345 further reduced in the High-Optimal1 case, and the combustion duration is reduced. Moreover, owing to the
346 effective management of the combustion phasing, the PPRR is kept well under the limit in the High-Optimal1 case,
347 as denoted in Fig. 10(c).
348

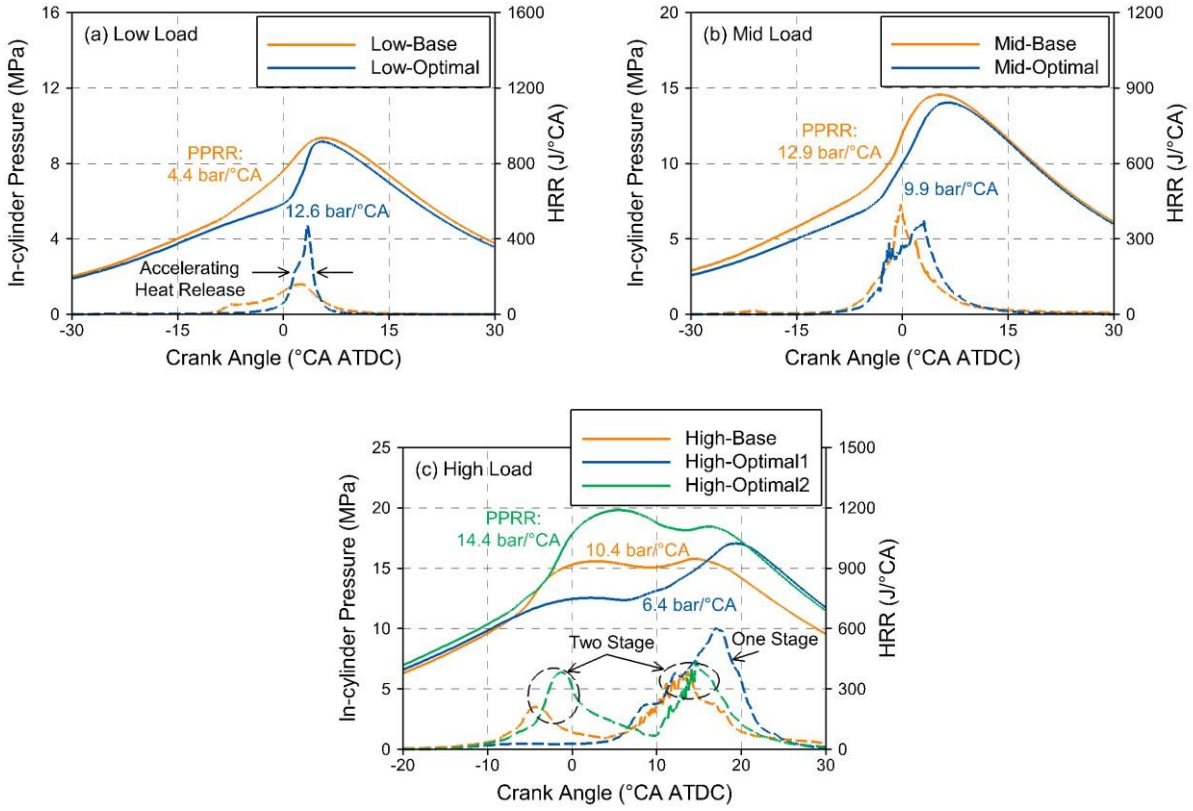

349
350

351 Fig. 10. Pressure and heat release rate of the optimal cases and baseline cases.
352

353 For further investigating the combustion characteristics at low and mid loads, Fig. 11 illustrates the
354 distribution of the in-cylinder temperature at 50% burn point (i.e., CA50) for the baseline and optimal cases. By
355 comparing Figs. 11(a1) and 11(a2), it can be found that, by utilizing a higher premix ratio, more homogeneous
356 combustion is accomplished with lower combustion temperature for the Low-Optimal case. This is beneficial to
357 decrease the NO_x and soot emissions (see Fig. 13(a)). By comparing Figs. 11(b1) and 11(b2) at mid load, it is found
358 that, for the Mid-Optimal case there exist two high-temperature (High-T) regions, and the local combustion
359 temperature is relatively higher than that of the Mid-Base case. This is because the Mid-Optimal case uses a lower

PR , thus a large amount of the diesel fuel is injected directly into the cylinder. Moreover, since a higher MF1 is used in the Mid-Optimal case, a larger amount of the diesel fuel concentrates above the piston lip, resulting in the high-reactivity and high-temperature region at this location. With the second injection, the fuel/air mixture in the piston bowl is ignited by the injected diesel. Thus, there are two separated combustion spots within the cylinder for the Mid-Optimal case, and the local combustion temperature is higher than that of the Mid-Base case. On the contrary, only one high-temperature region can be observed in the Mid-Base case, and the local temperature is relatively lower. It should be noted that the two high-reactivity regions reduce the requirement of high intake temperature, which is beneficial to decrease the heat transfer losses. However, NO_x emissions can be penalized to some extent. This will be explained in the following parts.

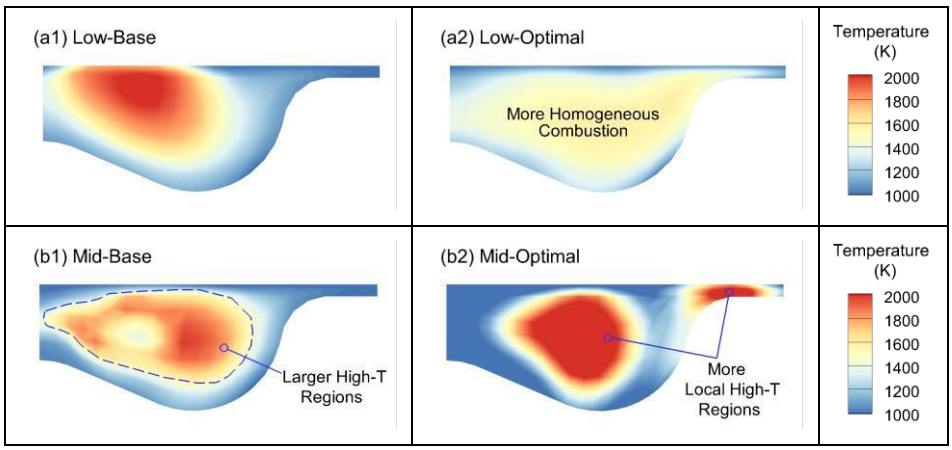

Fig. 11. In-cylinder distributions of temperature at CA50 for the baseline and optimal cases at low and mid loads.

In order to further explain the combustion behaviors at high load, Fig. 12 compares the in-cylinder equivalence ratio and temperature distributions in the combustion process for the baseline and optimal cases at high load. For the high-load cases, the combustion processes are more complex than that at low and mid loads, as illustrated in Fig. 10. To clearly illustrate the combustion behaviors, the time after the second direct injection event (SOI2) is chosen to be presented in Fig. 12. For the High-Base case, the in-cylinder combustion can be spatially spitted into two parts, *i.e.*, the homogeneous combustion and the diffusion combustion. The homogeneous

combustion corresponds to the first combustion stage from the premixed gasoline, and the diffusion combustion refers to the second combustion stage from the diesel injected after TDC (see Fig. 10(c)). It should be noted that since above 60% (energy fraction) of the fuel per cycle is from the injected diesel, the diffusion combustion occupies a large fraction in case High-Base. Moreover, since the gasoline reactivity is relatively lower, this combustion strategy needs a higher T_{ivc} to ensure the combustion of the premixed lean gasoline/air mixture. Thus, it is observed from Fig. 12(a) that the global combustion temperature is relatively higher in the High-Base case.

For the High-Optimal2 case, the combustion can still be splitted into two parts, *i.e.*, the premixed RCCI combustion and the diffusion combustion, as shown in Fig. 12(c). As mentioned above, a considerable amount of the diesel fuel is injected before -30 °CA ATDC in the first injection of the High-Optimal2 case (see Fig. 9(c)). The diesel provided in the first injection is mixed with premixed gasoline, leading to the premixed RCCI combustion, which induces the first combustion stage in the High-Optimal2 case. Moreover, since the diesel mass of the first injection of the High-Optimal2 case is significantly higher than that of the High-Optimal1 case, the first diesel injection penetrates closer to the cylinder wall for the High-Optimal2 case. This leads to the auto-ignition region closer to the cylinder wall as well. Then, with the second diesel injection, the diffusion combustion occurs. This corresponds to the second combustion stage in the High-Optimal2 case. It can be found that, compared to the High-Base case, a portion of diesel fuel is transferred from the diffusion combustion into the premixed RCCI combustion in the High-Optimal2 case.

For the High-Optimal1 cases shown in Fig. 12, the global equivalence ratio is relatively higher compared to the High-Base and High-Optimal2 cases, which is due to the higher PR used in the High-Optimal1 case. Similar to the High-Optimal2 case, the premixed RCCI combustion is accomplished by mixing the diesel fuel in the first injection with the premixed gasoline in the High-Optimal1 case. Then, the residual small-amount diesel fuel is

injected into the high-temperature region owing to the RCCI combustion. Thus, as illustrated in Fig. 12(b), the diffusion combustion of the diesel fuel in the second injection and the RCCI combustion occur simultaneously at the same location leading to the one-stage combustion of the High-Optimal1 case (see Fig. 10(c)). This shortens the combustion duration, which helps to increase the thermal efficiency. Moreover, by increasing the PR in the High-Optimal1 case, the heat released from the RCCI combustion is increased, and the diffusion combustion is weakened. Thus, high NO_x and soot emissions can be well prevented.

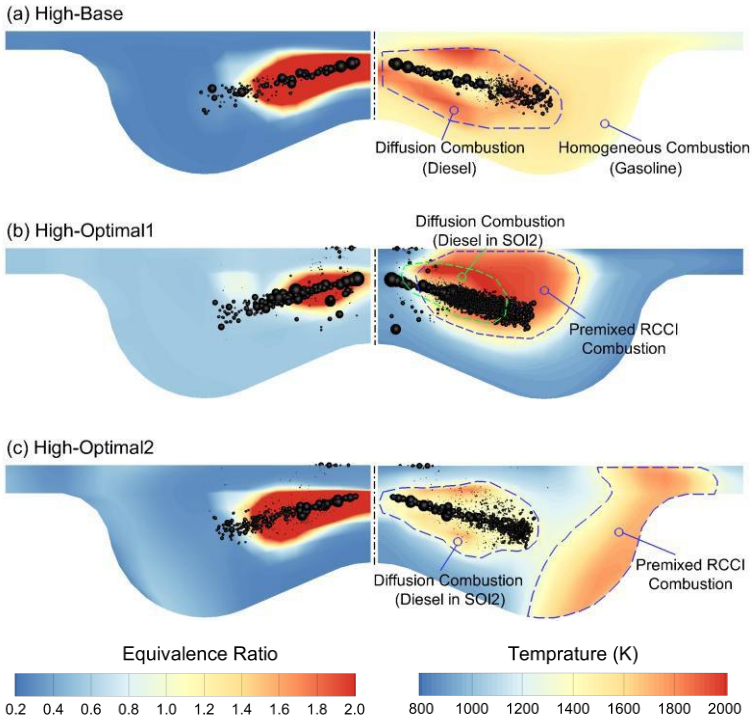

Fig. 12. Distributions of equivalence ratio and temperature after SOI2 (SOI for case High-Base) for the baseline and optimal cases at high load.

Fig. 13 summarizes the EISFC, NO_x and soot emissions of the optimal cases and baseline cases, which are the objectives of the optimization calculations. As can be seen in Fig. 13(a), at low load, the objectives are overall improved after optimization. This is because that the Low-Optimal case utilizes a higher PR and earlier fuel injections, leading to more homogeneous combustion with high heat release rate. Thus, the NO_x and soot emissions are reduced, while high fuel efficiency can be realized for the Low-Optimal case. At mid load, it can be found that

the EISFC and soot emissions of the Mid-Optimal case are considerably lower than those of the Mid-Base case, while the NO_x emissions are sacrificed to some extent. For EISFC, the fuel economy benefit is mainly resulted from the lower heat transfer losses of the Mid-Optimal case, which will be discussed in the next section. The soot reduction is mainly resulted from the relatively advanced fuel injections, which supplies more timing for the fuel/air mixing. The increase of NO_x emissions is owing to the local high combustion temperature and the two high-temperature regions, as mentioned above (see Fig. 11(b2)). However, in spite of the increase, the Euro 6 NO_x limit can still be satisfied, thus it is kept in the final optimal cases. At high load, the EISFC and NO_x emissions of the optimal cases are significantly lower than that of the High-Base case, while the soot emissions are decreased to some extent. The improvements are mainly due to the reduction of the diffusion combustion fraction, as mentioned above. Overall, according to Euro 6 emission regulations, both the soot and NO_x emissions of the optimal cases can meet the limits at each load.

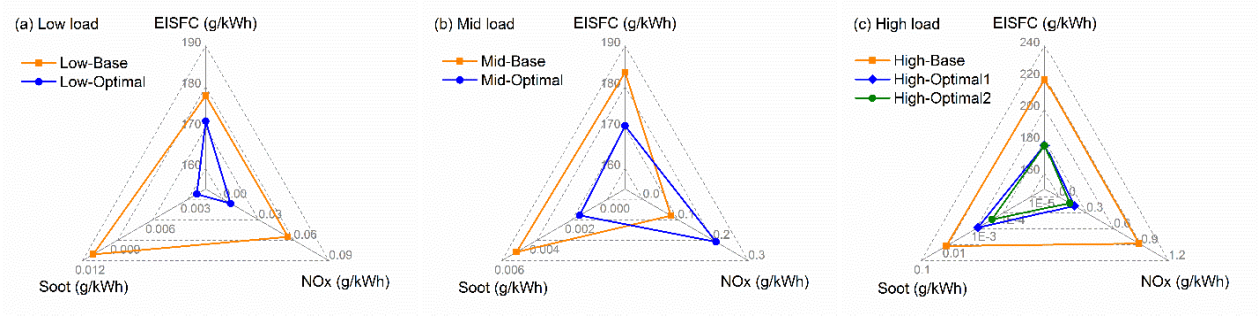

Fig. 13. Comparison of EISFC, NO_x and soot emissions between optimal cases and baseline cases.

3.2.3 Energy Analysis

For understanding the fuel efficiency benefits obtained from the optimization calculation, the energy analysis is performed in this section. Fig. 14 depicts the energy fractions of the optimal and baseline cases at each load. The energy fractions include the gross indicated work, heat transfer losses, exhaust losses, and incomplete combustion, which are represented by the blue, orange, green, and grey bars, respectively. Since the energy fraction of the

incomplete combustion is relatively low under the whole load range, the grey bars are not obviously presented in Fig. 14. As depicted in Fig. 14(a), the indicated work of the Low-Optimal case is slightly higher than that of the Low-Base case, indicating that the fuel efficiency is improved after the optimization. This is mainly due to the homogeneous combustion realized in the Low-Optimal case, which strengthens the combustion rate and shortens the combustion duration. Correspondingly, the constant-volume degree of the combustion process is increased. Thus, the indicated work is increased, while the heat transfer losses are decreased. Meanwhile, since the Low-Optimal case utilizes a higher T_{ivc}, the incomplete combustion is nearly eliminated. Thus, the fuel efficiency of the Low-Optimal case is higher than that of the Low-Base case. At mid load, the indicated work is increased after the optimization as well, as shown in Fig. 14(a). This is primarily owing to the reduction of the heat transfer losses, which will be discussed next. Besides, since a relatively lower PR is employed, the fraction of the incomplete combustion is slightly increased in the Mid-Optimal case.

At high load, it can be seen that both the High-Optimal1 and High-Optimal2 cases exhibit higher indicated work than the High-Base case due to the reduction of diffusion combustion. Because a large fraction of diffusion combustion exists in the High-Base case, the combustion duration is extremely long, as illustrated in Fig. 10(c). Thus, the constant-volume degree is reduced, leading to lower indicated work and fuel efficiency of the High-Base case. Meanwhile, the diffusion combustion results in significant post combustion, as shown in Fig. 10(c). Thus, the exhaust losses of the High-Base case are significantly higher compared to the High-Optimal1 and High-Optimal2 cases. Furthermore, by comparing the energy distributions of the baseline and optimal cases at high load, it is found that the heat transfer losses reduction also contributes to the improvement of the indicated work for the High-Optimal1 and High-Optimal2 cases. To explain the discrepancies in the heat transfer losses among the baseline and optimal cases at mid and high loads, the heat transfer process is further investigated.

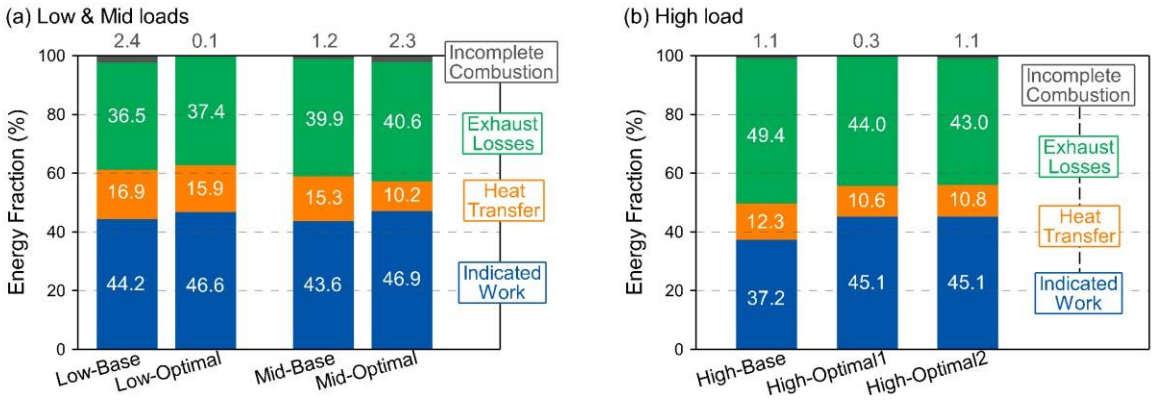

Fig. 14. Energy distributions of optimal cases and baseline cases.

Figs. 15(a) and 15(b) illustrate the temperature and heat transfer rate of the optimal and baseline cases at mid and high loads. As indicated by Gingrich et al. [37], the heat transfer losses can be decreased with lower combustion temperature and shortened combustion duration. From Figs. 15(a) and 15(b), it can be observed that since the combustion temperature of the Mid-Base and High-Base cases is higher than that of the optimal cases, a higher heat transfer rate is found for the two cases. Moreover, as mentioned above, the combustion duration is prolonged in the High-Base case due to the diffusion combustion, yielding further increasing the heat transfer losses. Therefore, compared to the optimal cases, the energy fraction of the heat transfer losses for the Mid-Base and High-Base cases are relatively higher, as shown in Fig. 14.

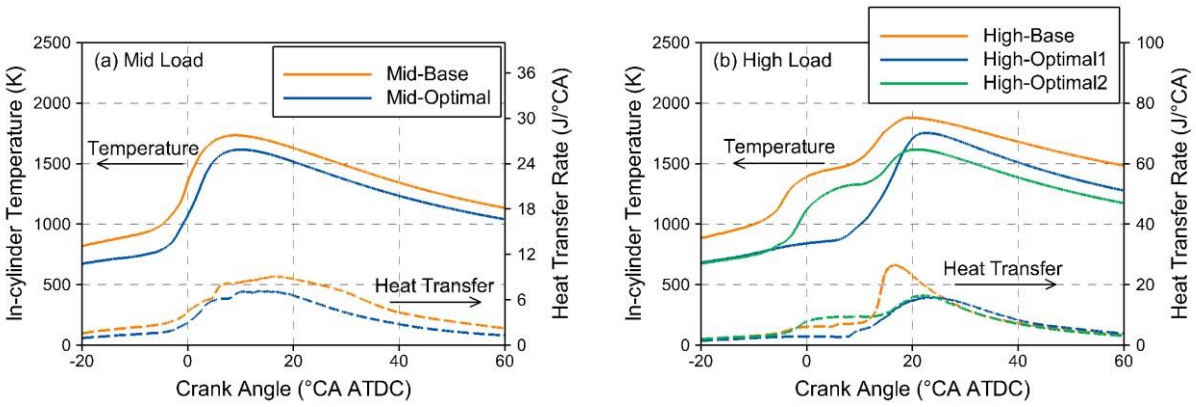

Fig. 15. Temperature and heat transfer rate of the optimal and baseline cases at mid load.

In addition, the lower combustion temperature of the optimal cases is also because that the optimized T_{ivc} is lower than that of the baseline cases at mid and high loads, as can be found in Fig. 8(b). At mid load, since a lower PR is employed in the Mid-Optimal case, more diesel fuel is provided towards direct injection. Thus, the reactivity of the in-cylinder charge is increased, and a lower T_{ivc} is needed to maintain an appropriate combustion phasing. At high load, since the premixed RCCI combustion plays a more dominant role in the optimal cases, the control of T_{ivc} is crucial. With the increased fuel mass at high load, the total input energy is elevated. Thus, a lower T_{ivc} is introduced to avoid the overly advanced combustion phasing, so that the PRR can be maintained under the limit. Therefore, it can be summarized that a lower T_{ivc} is beneficial for simultaneously decrease the heat transfer losses and manage the combustion phasing. However, owing to the introduction of the EGR and the higher exhaust gas temperature with increasing load, the cooling of the intake gases becomes very important.

4 Conclusions

Based on the diesel/gasoline dual-mode dual-fuel (DMDF) combustion concept, seven operating parameters with crucial influences on the engine performance and emissions were chosen as variables to be optimized by utilizing the genetic algorithm. The objective of this optimization study was to minimize the fuel consumption, NO_x and soot emissions simultaneously for the DMDF combustion. The major conclusions of the present study can be provided as follows.

1. As load increases, the fuel injection timings should be retarded, and the fraction of the first injection of the diesel fuel should be decreased to prohibit overly advanced combustion phasing. Meanwhile, the intake pressure should be increased to provide adequate fresh air for fuel oxidation with higher loads.
2. At low load, a higher T_{ivc} is needed to strengthen the combustion rate and increase the fuel efficiency. At mid and high loads, a lower T_{ivc} should be used for simultaneously decreasing the heat transfer losses and

controlling the combustion phasing. Moreover, the control of the intake temperature is very crucial for the stable operation of the DMDF combustion at wide load ranges.

3. At low load, simultaneous improvement of the fuel economy and emissions can be realized after the optimization due to the strengthening of the homogeneous combustion. At mid load, the fuel economy can be improved by reducing the heat transfer losses while NO_x emissions are sacrificed to some extent due to the local high-temperature regions. At high load, improved fuel economy and emissions can be realized by transferring a portion of diffusion combustion into premixed RCCI combustion.
4. By optimizing the operating parameters, the performance of the diesel/gasoline DMDF combustion strategy is considerably improved. Overall, the gross indicated thermal efficiency above 45% can be achieved, and the Euro 6 NO_x and soot emission standards can be satisfied in the test load range.

Acknowledgments

This work was partially supported by the National Natural Science Foundation of China (Grant Nos. 51961135105 and 91641117). The experimental results used in this investigation were obtained in a project funded by VOLVO Group Trucks Technology. The authors also acknowledge FEDER and Spanish Ministerio de Economía y Competitividad for partially supporting this research through TRANCO project (TRA2017-87694-R) and the Universitat Politècnica de València for partially supporting this research through Convocatoria de ayudas a Primeros Proyectos de Investigación (PAID-06-18).

Reference

[1] Johnson TV. Diesel emission control in review. SAE Technical Paper 2009-01-0121; 2009.

[2] Reitz RD, Duraisamy G. Review of high efficiency and clean reactivity controlled compression ignition (RCCI) combustion in internal combustion engines. Prog Energy Combust Sci 2015;46:12-71.

[3] Lim JH, Reitz RD. High load (21 bar IMEP) dual fuel RCCI combustion using dual direct injection. J Eng Gas Turbine Power 2014;136(10):101514(1-10).

[4] Splitter DA, Reitz RD. Fuel reactivity effects on the efficiency and operational window of dual-fuel compression ignition engines. Fuel 2014;118:163-75.

[5] Xu Z, Jia M, Li Y, Chang Y, Xu G, Xu L, Lu X. Computational optimization of fuel supply, syngas composition, and intake conditions for a syngas/diesel RCCI engine. Fuel 2018;234:120-34.

[6] D.F. Chuahy F, Kokjohn SL. Effects of the direct-injected fuel's physical and chemical properties on dual-fuel combustion. Fuel 2017;207:729-40.

[7] Murugesa Pandian M, Anand K. Comparison of different low temperature combustion strategies in a light duty air cooled diesel engine. Appl Therm Eng 2018;142:380-90.

[8] Li Y, Jia M, Chang Y, Kokjohn SL, Reitz RD. Thermodynamic energy and exergy analysis of three different engine combustion regimes. Appl Energy 2016;180:849-58.

[9] Tong L, Wang H, Zheng Z, Reitz R, Yao M. Experimental study of RCCI combustion and load extension in a compression ignition engine fueled with gasoline and pode. Fuel 2016;181:878-86.

[10] Agarwal AK, Singh AP, Maurya RK. Evolution, challenges and path forward for low temperature combustion engines. Prog Energy Combust Sci 2017;61:1-56.

[11] Dempsey AB, Walker NR, Gingrich E, Reitz RD. Comparison of low temperature combustion strategies

for advanced compression ignition engines with a focus on controllability. Combust Sci Technol 2014;186(2):210-41.

[12] Dempsey AB, Reitz RD. Computational optimization of reactivity controlled compression ignition in a heavy-duty engine with ultra low compression ratio. SAE Technical Paper 2011-24-0015; 2011.

[13] Hanson R, Curran S, Wagner R, Kokjohn S, Splitter D, Reitz R. Piston bowl optimization for RCCI combustion in a light-duty multi-cylinder engine. 2012; 2012-01-0380.

[14] Eichmeier J, Wagner U, Spicher U. Controlling gasoline low temperature combustion by diesel micro pilot injection. J Eng Gas Turbine Power 2012;134(7):072802(1-9).

[15] Molina S, García A, Pastor JM, Belarte E, Balloul I. Operating range extension of RCCI combustion concept from low to full load in a heavy-duty engine. Appl Energy 2015;143:211-27.

[16] Benajes J, García A, Monsalve-Serrano J, Boronat V. Achieving clean and efficient engine operation up to full load by combining optimized RCCI and dual-fuel diesel-gasoline combustion strategies. Energy Convers Manage 2017;136:142-51.

[17] Amsden AA. KIVA-3V: A block structured KIVA program for engines with vertical and canted valves. USA: Los Alamos National Laboratory Technical Report; LA-13313-MS, 1997.

[18] Wang BL, Lee CW, Reitz RD, Miles PC, Han Z. A generalized renormalization group turbulence model and its application to a light-duty diesel engine operating in a low-temperature combustion regime. Int J Engine Res 2012;14(3):279-92.

[19] Zhang Y, Jia M, Liu H, Xie M, Wang T, Zhou L. Development of a new spray/wall interaction model for diesel spray under PCCI-engine relevant conditions. Atomization Spray 2014;24(1):41-80.

[20] Zhang Y, Jia M, Liu H, Xie M. Development of an improved liquid film model for spray/wall interaction

under engine-relevant conditions. Int J Multiphase Flow 2016;79:74-87.

[21] Yi P, Long W, Jia M, Tian J, Li B. Development of a quasi-dimensional vaporization model for multi-component fuels focusing on forced convection and high temperature conditions. Int J Heat Mass Transfer 2016;97:130-45.

[22] Zhang Y, Jia M, Yi P, Liu H, Xie M. An efficient liquid film vaporization model for multi-component fuels considering thermal and mass diffusions. Appl Therm Eng 2017;112:534-48.

[23] Cao J, Jia M, Niu B, Chang Y, Xu Z, Liu H. Establishment of an improved heat transfer model based on an enhanced thermal wall function for internal combustion engines operated under different combustion modes. Energy Convers Manage 2019;195:748-59.

[24] Nordin PAN. Complex chemistry modeling of diesel spray combustion. Sweden: Chalmers University of Technology; 2001. PhD Thesis.

[25] Ricart LM, Reltz RD, Dec JE. Comparisons of diesel spray liquid penetration and vapor fuel distributions with in-cylinder optical measurements. J Eng Gas Turbine Power 2000;122(4):588-95.

[26] Kee RJ, Rupley FM, Meeks E, Miller JA. CHEMKIN-III: A FORTRAN chemical kinetics package for the analysis of gas phase chemical and plasma kinetics. USA: Sandia National Laboratory Technical Report; SAND96-8216, 1996.

[27] Chang Y, Jia M, Li Y, Xie M. Application of the optimized decoupling methodology for the construction of a skeletal primary reference fuel mechanism focusing on engine-relevant conditions. Front Mech Eng 2015;1:1-11.

[28] Xu G, Jia M, Li Y, Chang Y, Liu H, Wang T. Evaluation of variable compression ratio (VCR) and variable valve timing (VVT) strategies in a heavy-duty diesel engine with reactivity controlled compression

ignition (RCCI) combustion under a wide load range. Fuel 2019;253:114-28.

[29] Li Y, Jia M, Chang Y, Xu Z, Xu G, Liu H, Wang T. Principle of determining the optimal operating parameters based on fuel properties and initial conditions for RCCI engines. Fuel 2018;216:284-95.

[30] Benajes J, Pastor JV, García A, Monsalve-Serrano J. The potential of RCCI concept to meet EURO VI NOx limitation and ultra-low soot emissions in a heavy-duty engine over the whole engine map. Fuel 2015;159:952-61.

[31] Kim M, Reitz RD, Kong SC. Modeling early injection processes in HSDI diesel engines. SAE Technical Paper 2006-01-0056; 2006.

[32] Deb K, Pratap A, Agarwal S, Meyarivan T. A fast and elitist multiobjective genetic algorithm: NSGA-II. IEEE Trans Evol Comput 2002;6(2):182-97.

[33] Li Y, Jia M, Chang Y, Liu Y, Xie M, Wang T, Zhou L. Parametric study and optimization of a RCCI (reactivity controlled compression ignition) engine fueled with methanol and diesel. Energy 2014;65:319-32.

[34] Xu G, Jia M, Li Y, Chang Y, Wang T. Potential of reactivity controlled compression ignition (RCCI) combustion coupled with variable valve timing (VVT) strategy for meeting Euro 6 emission regulations and high fuel efficiency in a heavy-duty diesel engine. Energy Convers Manage 2018;171:683-98.

[35] Xu G, Jia M, Li Y, Xie M, Su W. Multi-objective optimization of the combustion of a heavy-duty diesel engine with low temperature combustion under a wide load range: (I) computational method and optimization results. Energy 2017;126:707-19.

[36] Leermakers CAJ, Somers LMT, Johansson BH. Combustion phasing controllability with dual fuel injection timings. SAE Technical Paper 2012-01-1575; 2012.

[37] Gingrich E, Ghandhi J, Reitz RD. Experimental investigation of piston heat transfer in a light duty engine under conventional diesel, homogeneous charge compression ignition, and reactivity controlled compression ignition combustion regimes. SAE Technical Paper 2014-01-1182; 2014